

Yohanes Edi Gunanto<sup>1,\*</sup>, Henni Sitompul<sup>1</sup>, Maya Puspitasari Izaak<sup>1</sup>, Yosef Sarwanto<sup>2</sup> & Wisnu Ari Adi<sup>2</sup>

<sup>1</sup>Department of Physics Education, Faculty of Education, University of Pelita Harapan,
Karawaci, Tangerang 15811, Indonesia

<sup>2</sup>Center for Research and Technology of Advanced Materials, National Research and
Innovation Agency, Tangerang Selatan 15314, Indonesia

\*E-mail: yohanes.gunanto@uph.edu

#### **Highlights:**

- Hexaferrite based materials can be applied as microwave absorbers (anti-radar).
- Substitution of Ba atoms and/or Fe atoms can increase reflection loss (RL) and bandwidth.
- Solid-state reaction synthesis by mechanical alloying with high energy milling is relatively cheap and easy compared to other methods.

**Abstract.** In this study, hexaferrite  $Ba_{0.95}La_{0.05}Fe_{12-2x}Zn_xTi_xO_{19}$  (x = 0; 0.5; and 1.0) was synthesized and characterized, which can be applied as microwave absorber in the X-band frequency range. It is a potential candidate for a radar absorbing material for microwave absorption, particularly for use in anti-radar paint in the defense sector. Samples were prepared using solid state reaction synthesis with high energy milling. After sintering at the right temperature, the samples were characterized using an X-ray diffractometer (XRD), a scanning electron microscope (SEM), a vibrating-sample magnetometer (VSM) and vector network analysis (VNA). The XRD characterization results indicated that all samples were in phase and had a hexagonal lattice structure with a P63/mmc space group and a crystallite size between 38 and 45 nm. The surface morphology of the characterization results using SEM showed a heterogeneous particle shape with particle sizes ranging from 140 to 200 nm. Substitution of Ti<sup>4+</sup> ions for Fe<sup>3+</sup> ions by Zn<sup>2+</sup> ions resulted in a decrease of the magnetic saturation (Ms), the magnetic remanence, and the sample's coercivity field. With a sample thickness of 1.5 mm, the VNA results confirmed that the ability to absorb microwaves and bandwidth will increase along with increase of the substitution value x. The reflection loss value was about -13.3 dB at a frequency of around 11 GHz, with a bandwidth of 1.4 GHz for the sample with x = 1.0 composition.

**Keywords**: Ba0.95La0.05Fe12-2xZnxTixO1; broadband; hexaferrite; high energy milling; microwave absorber; X-band.

#### 1 Introduction

Hexaferrite-based materials are of great interest to many researchers [1-8]. This is because they are very useful for many different uses, for example for microwave absorption [1-5,9-17] or electromagnetic interference (EMI) shielding [2,9,12]. Hexaferrite-based materials also have high permeability [6,12,18-19] and a high Curie temperature ( $\text{Tc} \approx 723 \text{ K}$ ) [12]. Previous research hasfound that barium-strontium hexaferrite is very applicable as a microwave absorber in the X-band frequency range from 8 to 12 GHz [20-23]. A problem that is still faced is that the bandwidth is narrow: around 1 GHz for a value of RL < -10 dB. Therefore, it is necessary to look for materials that can produce wider bandwidths.

Several different sample-making processes have been carried out, including:

- 1. Sol-gel the process of forming hexaferrite phase through a chemical reaction from nitrate-based raw material in a solution at low temperatures [1,3-6,9,18].
- 2. Hydrothermal hexaferrite phase formation via a solution reaction-based approach in a range from room temperature to very high temperatures [10,13,17].
- 3. Sonochemical hexaferrite phase formation by using strong ultrasonic radiation [11].
- 4. Solid-state reaction a chemical decomposition reaction of a heated mixture of solid compounds to produce a new solid composition [12,16,19,24].
- 5. Electrospinning the best method for producing nanofibers due to their versatility and easy sustainable production of nanofibers from a wide variety of materials [14].
- 6. Co-precipitation the classical and simplest method for synthesizing nanoparticles of oxide materials [15].

Combining barium/strontium hexaferrite-based microwave absorbers with rare earth metals is an interesting approach, mainly studied at the end of the previous decade. This is done by substitution in the position of Fe [1,3-5,10-11,13,18,24], in the barium/strontium position [14,16,19], or even at the same time in the position of Ba/Sr and Fe [6,9,15,17]. This is done to increase their capability as microwave absorber with a wide bandwidth but with the dimensions of the sample as thin as possible so that the sample will be as lightweight as possible. Mohammed, *et al.* obtained bandwidth values of 1.7 GHz (between 15.7 and 17.4 GHz) with a chemical composition of  $Ba_{1-x}Co_xFe_{12-x-y}Dy_xLa_yO_{19}$  and 3-mm sample thickness, for x = 0.3 and y = 0.6 [9]. With the same thickness  $BaLa_xGd_xFe_{12-2x}O_{19}$  actually has no bandwidth [4].

Zhao, et al. [3] varied the thickness of a BaFe<sub>11.92</sub>(La, Nd)<sub>0.04</sub>O<sub>19</sub>-TiO<sub>2</sub>/MCNTs/poly (3-methyl thiophene) composite sample to widen the bandwidth. The bandwidth increased with a sample thickness of 2 to 2.5 mm, whereas it decreased with a sample thickness of more than 2.5 mm. The largest bandwidth was 0.5 GHz and 1.0 GHz for the samples with a composition of 0.2: 0.25: 1.0, and 0.2: 0.20: 1.0, respectively. Goel, et al. obtained a bandwidthof 2.94 GHz for BaFe<sub>11.96</sub>Nd<sub>0.04</sub>O<sub>19</sub> with a thickness of 2.2 mm [5]. Some of the aresearch results above still leave problems regarding the smallest possible sample thickness with the greatest possible bandwidth. Because of this, the search for other compositions is still wide open.

Based on the research results of Taryana, *et al.* [25], the effect of La substitution can reduce the magnetocrystalline anisotropy constant to 1.29 x 10<sup>5</sup> erg/cm<sup>3</sup>. The single-phase La-doped barium hexaferrite sample had superior microwave characteristics over the undoped barium hexaferrite samples in the X-band frequency range. Meanwhile, Winatapura, *et al.* [26] found changes in magnetic properties such as magnetic coercivity, remanence, and magnetization saturation, which decreased with increased Zn-Ti substitution. The doping effect of Zn-Ti could increase microwave absorption at X-band frequencies. A material can only be used as a microwave absorbing material if it has both permeability and permittivity.

This is because microwaves have photon energy, which can polarize the magnetic and electrical properties of a material through the impedance matching mechanism. The magnetic properties of  $Ba_{0.95}La_{0.05}Fe_{12-2x}Zn_xTi_xO_{19}$  are affected by the magnetic dipole moment of the  $Fe^{3+}$  ions, while the electrical properties are controlled by the electric dipole moment of the  $La^{3+}$ ,  $Zn^{2+}$  and  $Ti^{4+}$  ions. Every two  $Fe^{3+}$  ions are replaced by one  $Zn^{2+}$  ion and one  $Ti^{4+}$  ion. This means that the contribution of the microwaves to increasing the material permittivity is affected by the two ions. Thus, referring to the results of the two previous studies, in this paper, a sample of  $Ba_{0.95}La_{0.05}Fe_{12-2x}Zn_xTi_xO_{19}$  (x=0;0.5; and 1.0) was prepared using the wet-milling solid-state reaction method and high energy milling. This technique has previously been used to synthesize nanomaterials or nanoquasicrystallines and is able to form one phase [7-8,20-23,25-26].

It does not only combine particles but is also able to reduce the particle size through a heating process to a point where a single phase can be formed. In addition, this milling technique is one of the cheapest available for large-scale production of nanoparticle size materials. The effects of the substitution of Zn<sup>2+</sup> and Ti<sup>4+</sup> ions for Fe<sup>3+</sup> ions with a thin sample thickness (1.5 mm) will be discussed below in terms of the structure, surface morphology, magnetization properties, reflection loss (RL), and the bandwidth of its microwave absorption capability.

## 2 Experiment

With stoichiometric calculations, samples of  $Ba_{0.95}La_{0.05}Fe_{12-2x}Zn_xTi_xO_{19}$  (x=0; 0.5; and 1.0) were made from a mixture of raw materials of  $BaCO_3$ ,  $La_2O_3$ ,  $Fe_2O_3$ , ZnO and  $TiO_2$ . The composition of the research materials was based on and improved from the research of Taryana, *et al.* [25] and Winatapura, *et al.* [26]. Each ingredient used was a product from Merck and had purity > 99%. The mixture of these materials was put in a stainless-steel vial together with iron balls with a weight ratio of 1:4 between the powder and the balls. The mixture was then milled in wet-milling condition at seven hundred and fifty turns per minute for 50 hours. The sample was then sintered at 1000 °C in the air for 5 hours.

The phases formed and the lattice structure were observed using a PAN Analytical Empyrean X-ray diffractometer (XRD) (Cu K $\alpha$ ,  $\lambda$  = 1.5406 Å). The XRD measurement data were then qualitatively and quantitatively analyzed using the GSAS (General Structure Analysis System) software to determine changes in the material structure parameters [27]. Characterization of the surface morphology using a JEOL JED 2300 scanning electron microscope (SEM) and an OXFORD VSM 1.2H vibrating-sample magnetometer (VSM) was done to measure the magnetic quantities, such as magnetic saturation (Ms), magnetic remnant (Mr), and coercivity field (Hc). Anritsu MS46322A type Vector Network Analysis (VNA) was used to measure the ability of the sample (1.5 mm thick) to absorb microwaves in the X-band frequency range.

## 3 Results and Discussion

The XRD diffraction patterns from the samples without substitution and with  $Zn^{2+}$ - $Ti^{4+}$  substitution can be seen in Figure 1(a). The results of refinement using the GSAS software are shown in Figure 1(b-d). The refinement results of the XRD pattern as shown in Figure 1 demonstrate a balance between the theoretical and the experimental data. The suitability parameters that must be met are fit criteria (wRp  $\leq$  0.1) and goodness of fit ( $\chi^2 \leq$  1.3) [27].

All samples were single phase. No other phases were detected. The crystal structure of all samples was hexagonal with a P63/mmc space group. The analysis results of the structural parameters, namely lattice parameters (a, b and c), unit cell volume (V), and atomic density ( $\rho$ ), are shown in Table 1. From the data, it can be assumed that substitution by  $Zn^{2+}$  and  $Ti^{4+}$  does not change the crystal structure but rather increases the unit cell volume. This result can be explained by the radius of the Fe<sup>3+</sup> ion (0.65 Å), the radius of the Zn<sup>2+</sup> ion (0.74 Å), and the radius of the Ti<sup>4+</sup> ion (0.60 Å) [28], resulting in the substitution of Zn<sup>2+</sup> and Ti<sup>4+</sup> ions for Fe<sup>3+</sup> ions, causing the lattice volume to increase from 697.2 Å<sup>3</sup> to 699.8 Å<sup>3</sup>.

Microwave Absorbing Material of Ba<sub>0.95</sub>La<sub>0.05</sub>Fe<sub>12-2x</sub>Zn<sub>x</sub>Ti<sub>x</sub>O<sub>19</sub> (x = 0; 0.5; and 1.0) with Broadband Characteristic at X-band Frequency

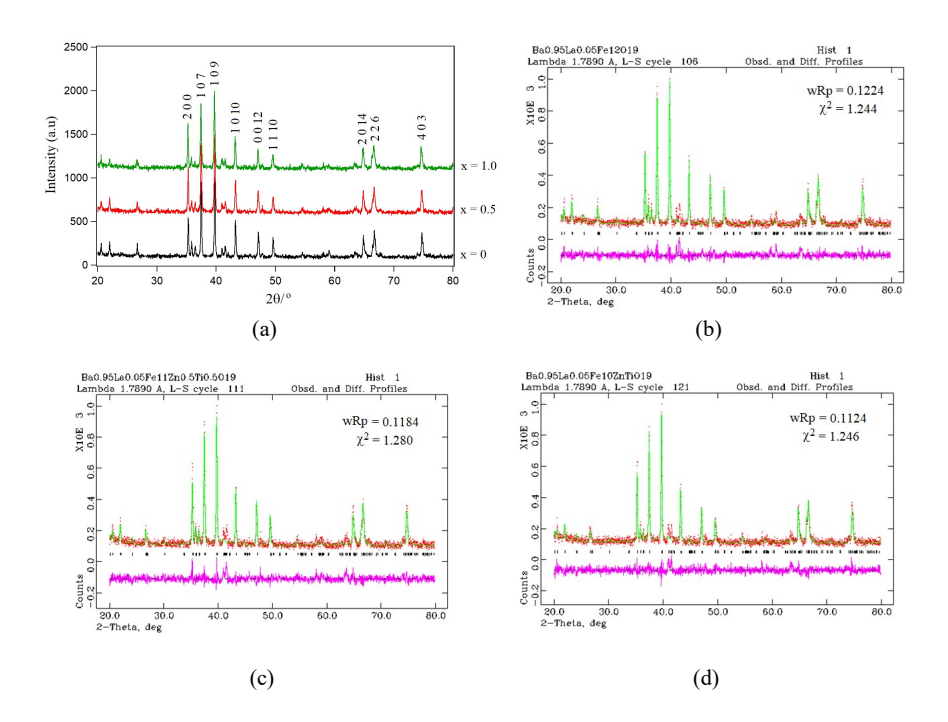


Figure 1 (a) XRD diffraction patterns for samples x = 0; 0.5; and 1.0 and results refined with the GSAS program (b) x = 0; (c) x = 0.5; and (d) x = 1.0.

**Table 1** Lattice parameters of  $Ba_{0.95}La_{0.05}Fe_{12-2x}Zn_xTi_xO_{19}$ .

x	a = b (Å)	c (Å)	c/a	vol. (ų)	ρ (g/cm³)
0	5.8910(3)	23.199(1)	3.938	697.2(1)	5.773
0.5	5.8950(3)	23.214(2)	3.938	698.6(1)	5.761
1.0	5.8985(3)	23.227(2)	3.938	699.8(1)	5.751

The lattice parameter value c increased from 23.199 Å to 23.227 Å, while the lattice parameter a = b remained almost constant. Similar results were also obtained by Baniasadi, *et al.* [29]. Some other studies indicate that the substitution of rare-earth metals, Nd<sup>3+</sup> [10], and La<sup>3+</sup> [14] on Ba<sup>2+</sup> do not change the crystal structure, i.e., the crystal structure remains hexagonal. The same results were obtained when La<sup>3+</sup> was substituted with Fe<sup>3+</sup> [9]. The heating process determines the phases formed. In this study, heating at a temperature of 1000 °C for 5 hours was able to produce a single phase. This process is more effective when compared with that of Ušák, *et al.* [12] and Guo, *et al.* [15], where

to obtain a single phase, a heating temperature of 1200 °C must be used for 6 hours and a heating temperature of 1250 °C for 5 hours, respectively. Mahmood, et al. [24] detected another phase (multiphase) for heating at 1200 °C for 2 hours.

The mean crystallite size and lattice strains of the single-phase samples were evaluated by means of a Williamson-Hall (W-H) plot of the peak width of the XRD pattern. The W-H plot is based on Eq. (1) [30]:

$$\beta \cos \theta = \frac{k\lambda}{D} + 4\varepsilon \sin \theta \tag{1}$$

where k,  $\lambda$ ,  $\theta$ , D,  $\beta$ , and  $\varepsilon$  are respectively a constant (0.9), the wavelength of the X-ray radiation, the Braggs diffraction angle, the mean crystallite size, a corrected value of full wave at half maximum (FWHM), and the lattice strain. The plot  $\beta$  cos  $\theta$  versus  $\sin \theta$  is used to obtain the value of lattice strain and mean crystallite size. The lattice strains are calculated from the ordinate interception at  $\sin \theta = 0$ . The mean crystallite size was obtained from the slope of the linear graph. The results from the analysis using the W-H method showed that the mean crystallite size of the samples for x = 0; 0.5; and 1.0 was about 38 nm, 40 nm, and 45 nm, respectively.

The surface morphology of the SEM results can be seen in Figure 2. The granular shape is still heterogeneous, with sizes ranging from 140 to 200 nm. This particle size was obtained by comparing the particle size with the scale. These results confirm that the three samples had a particle size consistency of about 140 to 200 nm and a crystallite size of 38 to 45 nm. The grain size was obtained by comparing the grain size with the scale. Essentially, Ti<sup>4+</sup> and Zn<sup>2+</sup> substitution does not affect the morphology and grain size distribution. Similar results have been obtained by Baniasadi, *et al.* [29]. Grain size is affected by milling time. A longer milling time will result in smaller particle sizes [31-32]. For a milling time of 16 hours, Mahmood, *et al.* [24] obtained grain sizes ranging from 200 to 1300 nm

The sample hysteresis curve of  $Ba_{0.95}La_{0.05}Fe_{12\cdot2x}Zn_xTi_xO_{19}$  with x=0; 0.5; and 1.0 can be seen in Figure 3. It appears that with the increase in the value of x, the magnetic saturation (Ms), magnetic remanence (Mr), and the coercivity field (Hc) decrease. The full results can be seen in Table 2. The decline in magnetic properties happened because the cations  $Ti^{4+}$  and  $Zn^{2+}$  are non-magnetic. Thus, this substitution will weaken the exchange interaction between the  $Fe^{3+}$  cations [29].

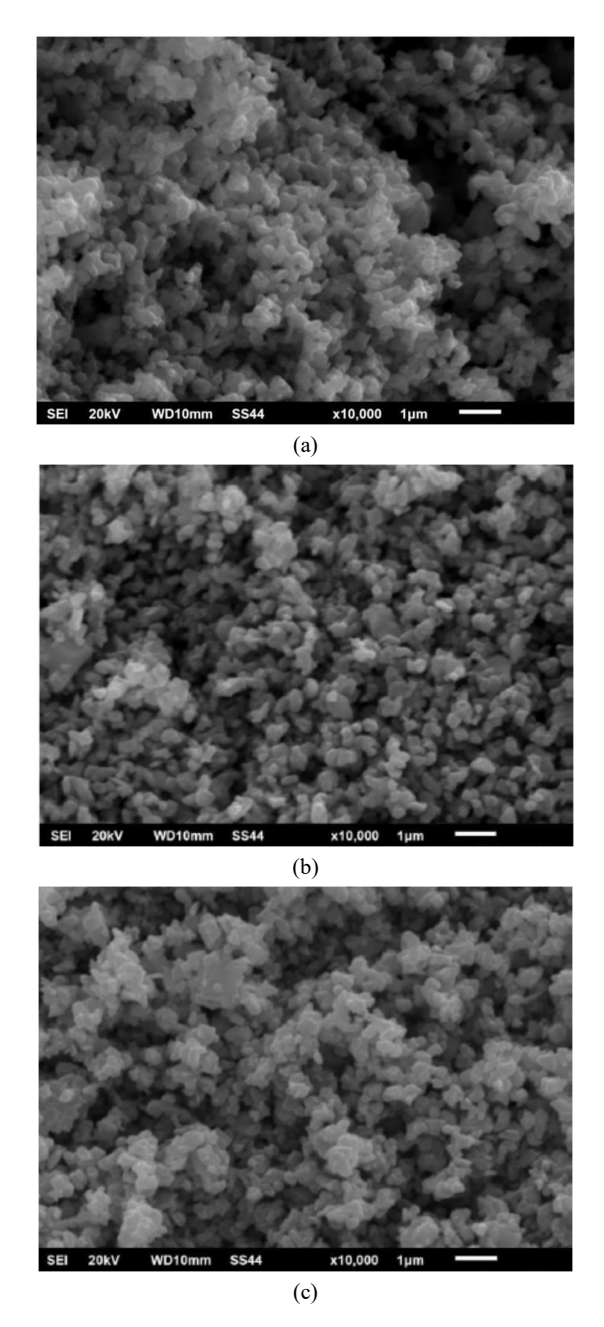


Figure 2 Surface morphology of SEM results for  $Ba_{0.95}La_{0.05}Fe_{12\text{-}2x}Zn_xTi_xO_{19}$  samples (a) x=0, (b) x=0.5, and (c) x=1.0.

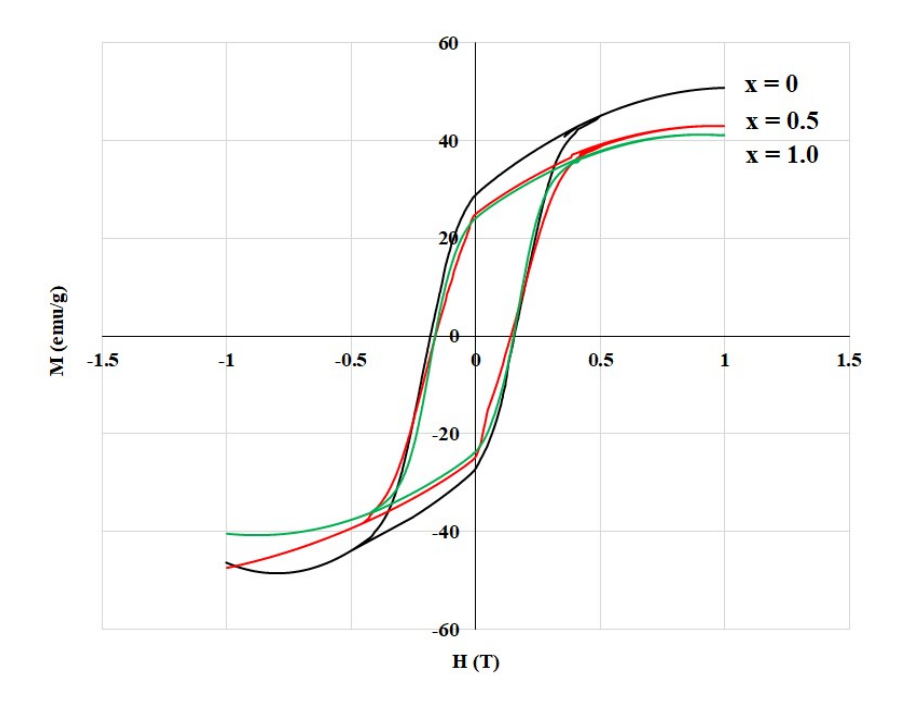


Figure 3 Hysteresis curve of sample  $Ba_{0.95}La_{0.05}Fe_{12-2x}Zn_xTi_xO_{19}$ .

Table 2 Summary of magnetic properties data Ba<sub>0.95</sub>La<sub>0.05</sub>Fe<sub>12-2x</sub>Zn<sub>x</sub>Ti<sub>x</sub>O<sub>19</sub>.

X	Ms	Mr	Нс	
	(emu/g)	(emu/g)	(T)	
0	50.76	28.83	0.18	
0.5	43.04	24.85	0.16	
1.0	41.08	23.95	0.16	

Generally, hexagonal ferrite is hard magnetic: it has a large amount of anisotropic energy. The energy from microwaves alone is not able to polarize magnetic spin moment the way hexagonal ferrite-based materials can. Because of this, material engineering is required so that the material's anisotropic field can be downsized into a semihard magnet but with a magnetic saturation that remains high. For this, the magnet's property changes need to be observed using VSM equipment. When material engineering is conducted, there are factors that affect microwave absorption. These factors are divided into intrinsic and extrinsic factors. Intrinsic factors include the internal factors of the material: the material has a complex permeability and permittivity. External factors include those that affect the effect of microwave propagation on the sample's geometric parameters (the particle's thickness, distribution, and size).

To show the absorption properties of a microwave, the reflection loss (RL) value is calculated based on Eqs. (2) and (3) [32]:

$$RL(dB) = 20 \log \left| \frac{(Z_{in} - 1)}{(Z_{in} + 1)} \right|$$
 (2)

$$Z_{in} = \left(\frac{\mu_r}{\varepsilon_r}\right)^{1/2} \tanh\left[j\left((2nfd)/c\right)(\mu_r\varepsilon_r)^{1/2}\right]$$
(3)

where  $Z_{in}$  is the input impedance of the absorber,  $\mu_r$  and  $\varepsilon_r$  are the permeability and relative permittivity of the medium, respectively, f is the frequency of the microwaves, d is the thickness of the absorber, and c is the speed of light.

Microwave propagation can be determined based on the value of the S-parameter. When the wave arrives, it hits the sample via a pair of adapters and the microwave will be reflected ( $S_{11}$ ) and transmitted ( $S_{21}$ ).  $S_{11}$  shows that the incoming waves from port 1 are reflected back to port 1, while  $S_{21}$  shows that the incoming waves from port 1 are transmitted and received by port 2. The microwave propagation equation uses the Nicholson-Ross-Weir (NRW) mathematical model [32-34]:

$$S_{11} = \frac{\Gamma(1 - T^2)}{1 - \Gamma^2 T^2}$$

$$S_{21} = \frac{T(1 - \Gamma^2)}{1 - \Gamma^2 T^2}$$
(4)

where  $\Gamma$  and T are the reflections of the transmission coefficient, respectively. Meanwhile, the percentage of microwave absorption can be determined as 100  $(1-\Gamma^2)$  (%).

**Table 3** Summary of Ba<sub>0.95</sub>La<sub>0.05</sub>Fe<sub>12-2x</sub>Zn<sub>x</sub>Ti<sub>x</sub>O<sub>19</sub> microwave absorption.

X	$\mathbf{Z}_{\mathbf{m}}$	Γ	RL (dB)	Absorption	Frequency	Bandwidth
	$(\Omega)$			(%)	(GHz)	(GHz)
0	33.2+j13.3	0.274	-11.5	92.5	10.7	0.9
0.5	31.6+j8.6	0.249	-12.1	93.8	10.9	1.0
1.0	34.8+j16.9	0.279	-11.1	92.2	9.3	0.8
1.0	35.1+j9.3	0.216	-13.3	95.3	11.0	1.4

Based on the Nicholson-Ross-Weir equation (Eqs. (2)-(4)), the factor that affects the absorption properties of microwaves is the  $S_{11}$  parameter, which is the reflection parameter. Parameter  $S_{21}$ , the transmission parameter, is not necessary in this case. Therefore, to ensure that no transmission factors would affect the measurements when conducting the measurement, the sample was placed on a metal surface. This meant that only two outcomes could emerge when the microwave was administered: the microwave was absorbed by the material or

was reflected by the metal. The adapter wave guide used had been calibrated with an impedance of 50  $\Omega$ . Generally, the material's absorption of the microwaves is caused by an impedance match between the microwaves and the material, which is achieved through the resonance mechanism.

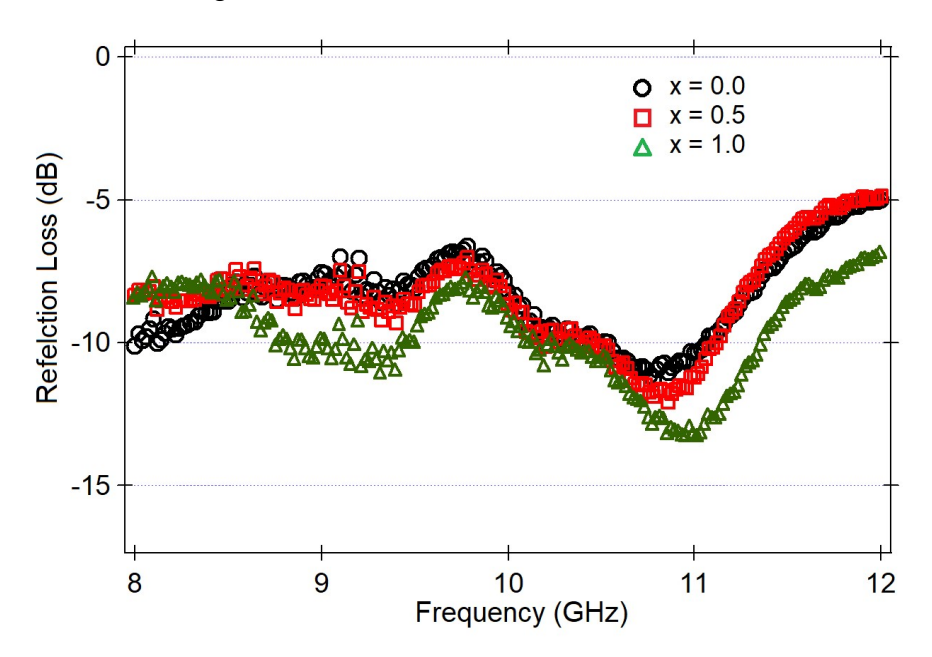


**Figure 4** Reflection loss curve of sample Ba0.95La0.05Fe12-2xZnxTixO19 for x = 0; 0.5; and 1.0.

The RL value produced as a frequency function for all samples of Ba<sub>0.95</sub>La<sub>0.05</sub>Fe<sub>12-2x</sub>Zn<sub>x</sub>Ti<sub>x</sub>O<sub>19</sub> (x = 0; 0.5; and 1.0) with a thickness of 1.5 mm in the frequency range from 8 GHz to 12 GHz is shown in Figure 4. It can be seen that for the x = 0 composition, the sample still showed a relatively low absorption characteristic for the given frequency. The maximum RL value was only -11.5 dB at a frequency of 10.7 GHz with a material impedance of  $Z_m = 33.2 + j13.3 \,\Omega$  and a reflection coefficient of 0.274. In addition, the material had a wide frequency bandwidth but one that was still relatively low (-8dB at a frequency of 0.9 GHz). The composition of x = 0.5 showed a better RL value compared to the x = 0 composition. With the x = 0.5 composition, the maximum RL value became -12.1 dB at a frequency of 10.9 GHz, with a material impedance of  $Z_m = 31.6 + j8.6 \,\Omega$  and a smaller reflection coefficient (0.249). This variant also had a wide absorption that was relatively large (-8.5 dB). However, the absorption frequency width relatively remained the same at 0.9 GHz. This means that the Zn<sup>2+</sup> and Ti<sup>4+</sup> elements are able to increase the microwave's absorption properties. Previous

studies featuring other elements achieved similar conclusions [3-5,13]. The x = 1 composition showed significant absorption changes in two different frequency areas in addition to an absorption increase in the same frequency areas as the x = 0 and x = 0.5 compositions. The maximum RL value increased to -13.3 dB at the 11.0 GHz frequency with an impedance of  $Z_m = 35.1 + j9.3~\Omega$  and a reflection coefficient that was also smaller (0.216). The material also had a larger absorption area, -10.0 dB, compared to the absorption area of the x = 0.5 composition. The frequency bandwidth also became wider (1.4 GHz). However, a second maximum RL value of -11.1 dB emerged at a frequency of 9.3 GHz, with an impedance of  $Z_m = 34.8 + j16.9~\Omega$ , a reflection coefficient of 0.279, and a relatively wide absorption bandwidth of -8.5 dB, with an absorption frequency of 0.8 GHz. The results of all test samples of  $Ba_{0.95}La_{0.05}Fe_{12-2x}Zn_xTi_xO_{19}$  (x = 0; 0.5; and 1.0) samples are summarized in Table 3.

These results indicate that the material Ba<sub>0.95</sub>La<sub>0.05</sub>Fe<sub>12-2x</sub>Zn<sub>x</sub>Ti<sub>x</sub>O<sub>19</sub> (x = 0; 0.5; and 1.0) can be considered a potential microwave absorber, particularly in antiradar paintin the defense sector. To act as a radar absorbing material, a material should not only have a high absorption, but also absorb in a broad frequency range. The material examined fulfills both requirements. This means that if there is a material with a high absorption rate and a wide bandwidth, enemy radar of any frequency, will be absorbed by the material as long as it is within the range of military radar (the X-band). This material was shown to be able to absorb 90% of microwaves at frequencies of 8.5 to 9.5 GHz and 10 to 11.5 GHz.

## 4 Conclusion

 $Ba_{0.95}La_{0.05}Fe_{12-2x}Zn_xTi_xO_{19}$  samples (x = 0; 0.5; and 1.0) were successfully synthesized using the solid-state reaction method with high energy milling. The substitution of  $Zn^{2+}$  and  $Ti^{4+}$  ions for  $Fe^{3+}$  ions does not change the crystal structure, which is hexagonal. Heterogeneous granules sizes ranged from 140 to 200 nm. The greater the value of x, the smaller the magnetic properties. With a thin sample (about 1.5 mm), the best result was -13.3 dB microwave absorption at a frequency of around 11 GHz with a bandwidth of 1.4 GHz, which means the material can be applied as a microwave absorber.

## Acknowledgments

This work was supported by Universitas Pelita Harapan Grants 2019 No. RInG-001-FIP/IX/2019 for the development of rare earth metal-based anti-radar magnetic materials.

#### References

- [1] Kanwal, M., Ahmad, I., Meydan, T., Cuenca, J.A., Williams, P.I., Farid, M.T. & Murtaza, G., Structural, Magnetic and Microwave Properties of Gadolinium-Substituted Ca-Ba M-Type Hexagonal Ferrites, Journal of Electronic Materials, 47, pp. 5370-5377, 2018.
- [2] Stergiou, C.A. & Litsardakis, G., Rare Earth Substituted Hexagonal Ferrites for Electromagnetic Absorber Applications. Recent Advances and Critical Issues, Journal of Surfaces and Interfaces of Materials, 2, pp. 79-87, 2014.
- [3] Zhao, J., Yu, J., Xie, Y., Le, Z., Hong, X., Ci, S., Chen, J., Qing, X., Xie, W. & Wen, Z., Lanthanum and Neodymium Doped Barium Ferrite-TiO<sub>2</sub>/MCNTs/poly (3-methyl thiophene) Composites with Nest Structures: Preparation, Characterization and Electromagnetic Microwave Absorption Properties, Scientific Reports, 6, 20496, 2016.
- [4] Abdollahi, F., Yousefi, M., Hekmati, M., Khajehnezhad, A. & Afghahi, S.S.S., *Magnetic and Microwave Absorption Properties of Barium Hexaferrite Doped with La*<sup>3+</sup> and Gd<sup>3+</sup>, Nanostruct, **9**(3), pp. 579-586, 2019.
- [5] Goel, S., Garg, A., Gupta, R.K., Dubey, A., Prasad, N.E. & Tyagi, S., Effect of Neodymium Doping on Microwave Absorption Property of Barium Hexaferrite in X-band, Mater. Res. Express, 7, 016109, 2020.
- [6] Want, B. & Bhat, B.H., Magnetic and Dielectric Characteristics of Nd and Nd-Mg Substituted Strontium Hexaferrite, J. Modern Electronic Materials 4(1), pp. 21-29, 2018.
- [7] Gunanto, Y.E., Cahyadi, L. & Adi, W.A., Effect of Mn and Ti Substitution on the Reflection Loss Characteristic of  $Ba_{0.6}Sr_{0.4}Fe_{11-z}MnTi_zO_{19}$  (z = 0, 1, 2 and 3), AIP Conference Proceedings, 1725, 020023, 2016.
- [8] Gunanto, Y.E., Cahyadi, L. & Adi, W.A., *Influence of Ti Addition on the Microwave Absorbing Behavior of Ba*<sub>0.6</sub>*Sr*<sub>0.4</sub>*Fe*<sub>12-X</sub>*ti*<sub>x</sub>o<sub>19</sub> *System at X-Band Frequencies*, Journal of Physics: Conf. Series, **1091**, 012009, 2018.
- [9] Mohammed, J., Carol T.T., Hafeez, H.Y., Basandrai, D., Bhadu, G.R Godara, S.K., Narang, S.B. & Srivastava, A.K., *Electromagnetic interference (EMI) Shielding, Microwave Absorption, and Optical Sensing Properties of BaM/CCTO Composites in Ku-band*, Results in Physics, 13, 102307, 2019.
- [10] Sharma, V., Kumari, S. & Kuanr, B.K., Rare Earth Doped M-type Hexaferrites; Ferromagnetic Resonance and Magnetization Dynamics, AIP ADVANCES, 8, 056232, 2018.
- [11] Almessiere, M.A., Slimani, Y., Demir Korkmaz, A., Baykal, A., Güngünes, H., Sözeri, H., Shirsath, S.E., Güner, S., Akhtar, S. & Manikandan, A., Impact of La<sup>3+</sup> and Y<sup>3+</sup> Ion Substitutions on Structural, Magnetic and Microwave Properties of Ni<sub>0.3</sub>Cu<sub>0.3</sub>Zn<sub>0.4</sub>Fe<sub>2</sub>O<sub>4</sub> Nanospinel

- Ferrites Synthesized via Sonochemical Route, RSC Adv., 9, pp. 30671-30684, 2019.
- [12] Ušák, E., Ušáková, M., Dosoudil, R., Šoka, M. & Dobročka, E., *Influence of Iron Substitution by Selected Rare-Earth Ions on the Properties of Nizn Ferrite Fillers and PVC Magneto-Polymer Composites*, AIP ADVANCES **8**, 047805, 2018.
- [13] Neelima, P. & Murthy, S.R., Effect of Dy<sup>3+</sup> Substitution on Microwave Behaviour of Nanocrystalline Mn-Zn Ferrite, Advanced Materials Proceedings, **3**(7), pp. 464-468, 2018.
- [14] Ju Li, C., Wang, B. & Na Wang, J. Magnetic and Microwave Absorbing Properties of Electrospun Ba<sub>(1-x)</sub> LaxFe<sub>12</sub>O<sub>19</sub> Nanofibers, Journal of Magnetism and Magnetic Materials, **324**, pp. 1305-1311, 2012.
- [15] Jing, W., Hong, Z., Bai, S., Ke, C. & Changrui, Z., *Microwave Absorbing Properties of Rare-Earth Elements Substituted W-type Barium Ferrite*, Journal of Magnetism and Magnetic Materials **312**(2), pp. 310-313, 2007.
- [16] Guo, F., Ji, G., Xu, J., Zou, H., Gan, S. & Xu, X., Effect of Different Rare-Earth Elements Substitution on Microstructure and Microwave Absorbing Properties of Ba<sub>0.9</sub>RE<sub>0.1</sub>Co<sub>2</sub>Fe<sub>16</sub>O<sub>27</sub> (RE=La, Nd, Sm) Particles, Journal of Magnetism and Magnetic Materials, **324**(6), pp. 1209-1213, March 2012.
- [17] Torabi, Z., Arab, A. & Ghanbari, F., Structural, Magnetic and Microwave Absorption Properties of Hydrothermally Synthesized (Gd, Mn, Co) Substituted Ba-Hexaferrite Nanoparticles, Journal of Electronic Materials, 47(2), 2018.
- [18] Unal, B., Almessiere, M., Slimani, Y., Baykal, A., Trukhanov, A.V. & Ercan, I., *The Conductivity and Dielectric Properties of Neobium Substituted Sr-Hexaferrites*, Nanomaterials, **9**, 1168, 2019.
- [19] Purwanto, P., Yunasfi & Mulyawan, A., *The Influence of Sintering Temperature on The Crystal Structure, Electric and Magnetic Properties of Ba*<sub>(2-x)</sub>*Nd*<sub>(x)</sub>*Fe*<sub>2</sub>*O*<sub>5</sub> *Composite,* Malaysian Journal of Fundamental and Applied Sciences, **15**(3), pp. 372-376, 2019.
- [20] Gunanto, Y.E., Sarwanto, Y. & Adi, W.A., Analysis of Crystallography Structure and Magnetic Properties of Microwave Absorbing Material Ba<sub>0.6</sub>Sr<sub>0.4</sub>Fe<sub>12-3x</sub>Zn<sub>2x</sub>Ti<sub>x</sub>O<sub>19</sub> (x = 0, 0.2, 0.4, and 0.6), Key Engineering Materials, **855**, pp. 293-298, 2020. DOI: 10.4028/www.scientific.net/KEM.855.293.
- [21] Gunanto, Y.E., Jobiliong, E. & Adi, W.A., *Microwave Absorbing Properties of Ba*<sub>0.6</sub> $Sr_{0.4}Fe_{12-z}Mn_zO_{19}$  (z=0-3) *Materials in X-Band Frequencies*, J. Math. Fund. Sci., Vol. 48, No. 1, pp. 55-65, 2016.
- [22] Gunanto, Y.E., Izaak, M.P., Sitompul, H. & Adi, W.A., Reflection Loss Characteristic as Coating Thickness Function on the Microwave Absorbing Paint at a Frequency of 8-12 GHz, IOP Conf. Series: Materials Science and Engineering, 515, 012074, 2019.

- [23] Gunanto, Y.E., Izaak, M.P., Sitompul, H. & Adi, W.A., Composite Paint based on Barium-Strontium-Hexaferrite as an Absorber of Microwave at X-band Frequency, Materials Today: Proceedings, 13, pp. 1-4, 2019.
- [24] Mahmood, S.H., Awadallah, A.M., Bsoul, I. & Maswadeh, Y., *Structural and Magnetic Properties of Lightly Doped M-type Hexaferrites*, arXiv:1707.04709 [cond-mat.mtrl-sci], 2017.
- [25] Taryana, Y., Adi, W.A., Mahmudin, D., Wahyu, Y. & Manaf, A., Structural, Magnetic and Microwave Absorption Characteristics of Ba<sub>1-x</sub>La<sub>x</sub>Fe<sub>12</sub>O<sub>19</sub> (x = 0; 0.1; 0.2;0.3;0.5;0.7), Key Engineering Materials, Vol. 855, pp. 261-267, 2020. DOI: 10.4028/www.scientific.net/KEM.855.261.
- [26] Winataputra, D.S., Ujiyanti, T.L & Adi, W.A., The Structure, Magnetic and Absorption Properties of Zn-Ti Substituted Barium-Strontium Hexaferrite Prepared by Mechanochemical Process, IOP Conf. Series: Materials Science and Engineering, 202, 012090, 2017. DOI:10.1088/1757-899X/202/1/012090.
- [27] Toby, B.H., EXPGUI, A Graphical User Interface for GSAS, J. Appl. Crystallogr, **34**, pp. 210-221, 2001.
- [28] Shannon, R.D., Revised Effective Ionic Radii and Systematic Studies of Interatomic Distances in Halides and Chalcogenides, Acta Cryst., A32, pp. 751-767, 1976.
- [29] Baniasadi, A., Ghasemi, A., Ghadikolaei, M.A., Nemati A. & Paimozd, E., Microwave Absorption Properties of Ti-Zn Substituted Strontium Hexaferrite, J Mater Sci: Mater Electron, 27, pp. 1901-1905, 2016.
- [30] Kumar, S., Supriya, S., Pradhan, L.K. & Kar, M., Effect of Microstructure on Electrical Properties of Li and Cr Substituted Nickel Oxide, J. Mater. Sci.: Mater. Electron. 28, 16679, 2017.
- [31] Gunanto, Y. E., Izaak, M.P., Silaban, S.S. & Adi, W.A., Effect of Milling Time on Microwave Absorption Ability on Barium-Hexaferrite Nanoparticles, Journal of Physics: Conf. Series, 1011, 012058, 2018.
- [32] Adi, W.A., Yunasfi., Mashadi, Winatapura, D.S., Mulyawan, A., Sarwanto, Y., Gunanto, Y.E. & Taryana, Y., 15 May 2019, Book: Electromagnetic Fields and Waves, *Metamaterial: Smart magnetic Material for Microwave Absorbing Material*, pp. 158-176, Publisher IntechOpen, UK, 2019. DOI: 10.5772/intechopen.84471.
- [33] Yaw, K.C., *Measurement of Dielectric Material Properties* (Rohde & Schwarz), Meas. Tech., pp. 1-35, 2006.
- [34] You K.Y., Lee Y.S., Zahid L., Malek M. F.A., Lee K.Y.& Cheng E.M., Dielectric Measurements for Low-loss Materials Using Transmission Phase-shift Method, Jurnal Teknologi, 77(10), pp. 69-77, 2015.